Analysis of Discontinuities in an Asymmetric Dielectric Slab Waveguide by Combination of Finite and Boundary Elements

Koichi Hirayama, *Member, IEEE,* and Masanori Koshiba, *Senior Member, IEEE*

***Abstract*—An approach that combines the finite-element and boundary-element methods is extended to the analysis of discontinuities in an asymmetric slab waveguide. The discontinuity region is divided into three regions. One is a finite region with arbitrary inhomogeneities, and the others are semi-infinite and homogeneous regions. The finite-element and boundary-element methods are applied to the former and latter regions, respectively. For uniform waveguide regions connected to discontinuities, analytical solutions are used, in which all the eigenmodes, namely guided modes, substrate radiation modes, and substrate-cover radiation modes are taken into account. To show the validity and usefulness of this approach, computed results are given for three kinds of step-discontinuities with TE and TM mode incidences.**

I. Introduction

SINCE an optical waveguide is in general made up of three dielectric layers called cover, film, and substrate, it is very important to analyze discontinuities in an asymmetric planar dielectric waveguide. However, there are few theoretical methods for the solution of the discontinuities. One of the reasons is that the asymmetric waveguide has complicated eigenmodes consisting of guided modes, substrate radiation modes, and substrate-cover radiation modes. The nature and behavior of these modes are detailed in Chapter 1 of [1]. An approach proposed by V. Ramaswamy and P. G. Suchoski, Jr. [2] takes transmitted guided modes, substrate radiation modes, and the propagating part of substrate-cover radiation modes into account, but ignores reflected guided modes and the nonpropagating part of substrate-cover radiation modes.

For discontinuities in a dielectric waveguide, we have proposed an approach based on a combination of the finite-element and boundary-element methods (CFBEM) [3], [4], and have confirmed that the CFBEM is very useful for arbitrarily shaped discontinuities. However, the approach is limited to discontinuities in a symmetric slab waveguide.

Manuscript received February 5, 1991; revised November 25, 1991. This work was partially supported by a Scientific Research Grant-in-Aid from the Ministry of Education, Science and Culture, Japan.

K. Hirayama is with the Department of Electronic Engineering, Kushiro National College of Technology, Kushiro, 084 Japan.

M. Koshiba is with the Department of Electronic Engineering, Hokkaido University, Sapporo, 060 Japan.

IEEE Log Number 9106053.

In this paper, we extend the CFBEM to the analysis of discontinuities in an asymmetric slab waveguide. Here, all the eigenmodes in the waveguide are taken into account. To show the validity and usefulness of this approach, computed results are given for three kinds of step-discontinuities with TE and TM mode incidences.

II. Basic Equations

Consider an asymmetric planar dielectric waveguide as shown in Fig. 1. The boundaries $\Gamma_0^{(+)}$ and $\Gamma_0^{(-)}$ are placed at infinity ($y = \pm\infty$) and the boundary

$$\Gamma_i = \Gamma_{iF} + \Gamma_{iB}^{(+)} + \Gamma_{iB}^{(-)} \qquad (i = 1, 2)$$

connects the discontinuity region to the uniform waveguide i, where d_i and $n_{ij}(j = 1, 2, 3)$ are the thickness and the refractive index of waveguide $i(n_{i2} > n_{i1} > n_{i3})$, respectively. The region Ω_F surrounded by the boundary

$$\Gamma_F = \Gamma_{1F} + \Gamma_{2F} + \Gamma_3^{(+)} + \Gamma_3^{(-)}$$

completely encloses the discontinuity region, the region $\Omega_B^{(+)}$ is surrounded by the boundaries

$$\Gamma_B^{(+)} = \Gamma_{1B}^{(+)} + \Gamma_{2B}^{(+)} + \Gamma_3^{(+)}$$

and $\Gamma_0^{(+)}$, and the region $\Omega_B^{(-)}$ is surrounded by the boundaries

$$\Gamma_B^{(-)} = \Gamma_{1B}^{(-)} + \Gamma_{2B}^{(-)} + \Gamma_3^{(-)}$$

and $\Gamma_0^{(-)}$.

Assuming that there is no variation of fields and refractive indices in the horizontal transverse z direction (see Fig. 1), we consider the following basic equation for harmonic wave propagation in the x direction:

$$\frac{1}{p}\left(\frac{\partial^2\phi}{\partial x^2} + \frac{\partial^2\phi}{\partial y^2}\right) + k_0^2 q\phi = 0 \tag{1}$$

where

$$\phi = E_z \quad p = 1 \quad q = n^2 \qquad \text{for TE modes} \tag{2a}$$

$$\phi = H_z \quad p = n^2 \quad q = 1 \qquad \text{for TM modes} \tag{2b}$$

$$k_0 = 2\pi/\lambda. \tag{3}$$

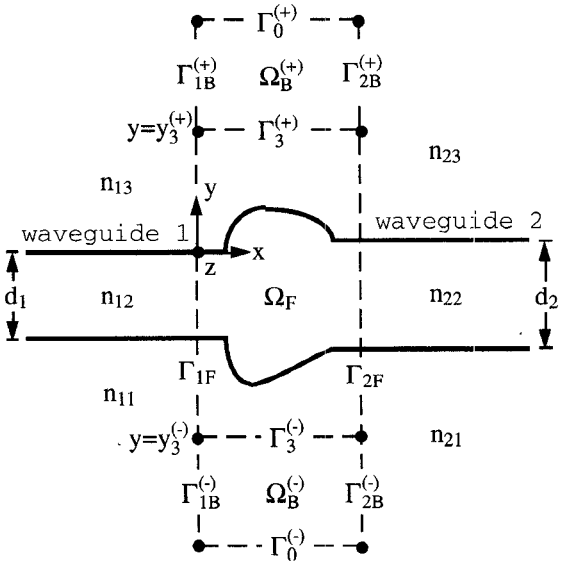

Fig. 1. Longitudinal cross-section of asymmetric planar dielectric waveguide.

Here E_z and H_z are the z components of the electric and magnetic fields, respectively, and λ is the wavelength of a plane wave in free space.

Since the normal derivative of ϕ on Γ_1, Γ_2, $\Gamma_3^{(+)}$, and $\Gamma_3^{(-)}$ appears in the finite element, boundary element, and analytical approaches which will be presented in the next section, in advance we define a function ψ proportional to it as follows:

$$\psi = -\lambda \partial\phi/\partial x \quad \text{on } \Gamma_1 \tag{4a}$$

$$\psi = \lambda \partial\phi/\partial x \quad \text{on } \Gamma_2 \tag{4b}$$

$$\psi = -\lambda \partial\phi/\partial y \quad \text{on } \Gamma_3^{(+)} \tag{4c}$$

$$\psi = \lambda \partial\phi/\partial y \quad \text{on } \Gamma_3^{(-)}. \tag{4d}$$

III. Mathematical Formulation

A. Finite Element Approach for Ω_F

Dividing the region Ω_F into a number of quadratic triangular elements, using a Galerkin procedure on (1), considering the contributions of all elements, and eliminating internal variables, namely the nodal points in Ω_F except Γ_F, we obtain the following small-sized matrix equation:

$$[A]\{\phi\}_F = [B]\{\psi\}_F \tag{5}$$

where the components of the $\{\phi\}_F$ and $\{\psi\}_F$ vectors are the values of ϕ and ψ at the nodal points on Γ_F, respectively.

B. Boundary Element Approach for $\Omega_B^{(+)}$ and $\Omega_B^{(-)}$

Applying the BEM with quadratic line element to the regions $\Omega_B^{(+)}$ and $\Omega_B^{(-)}$, and considering the radiation condition on $\Gamma_0^{(+)}$ and $\Gamma_0^{(-)}$, we obtain the following matrix equations:

$$[H]^{(+)}\{\phi\}_B^{(+)} = [G]^{(+)}\{\psi\}_B^{(+)} \quad \text{in } \Omega_B^{(+)} \tag{6a}$$

$$[H]^{(-)}\{\phi\}_B^{(-)} = [G]^{(-)}\{\psi\}_B^{(-)} \quad \text{in } \Omega_B^{(-)} \tag{6b}$$

where the components of the $\{\phi\}_B^{(\pm)}$ and $\{\psi\}_B^{(\pm)}$ vectors are the values of ϕ and ψ at the nodal points on $\Gamma_B^{(\pm)}$, respectively.

C. Analytical Approach

Assuming that the fundamental mode ($m = 0$) of unit amplitude is incident from the left side of waveguide 1 in Fig. 1, ϕ on Γ_i ($i = 1, 2$) may be expressed analytically as

$$\{\phi\}_i = \delta_{i1}\{f\}_1 + [Z]_i\{\psi\}_i \tag{7}$$

where

$$\{f\}_1 = 2\{f_0\}_1 \tag{8a}$$

$$\begin{aligned}[Z]_i = &\sum_{m=0}^{M_i-1} \frac{1}{-j\beta_{im}\lambda}\{f_m\}_i\{\hat{g}_m\}_i^T \\ &+ \int_0^{k_0\sqrt{n_{i1}^2-n_{i3}^2}} \frac{1}{-j\beta_i(\rho)\lambda}\{f^{(0)}(\rho)\}_i\{\hat{g}^{(0)}(\rho)\}_i^T d\rho \\ &+ \int_{k_0\sqrt{n_{i1}^2-n_{i3}^2}}^{\infty} \frac{1}{-j\beta_i(\rho)\lambda} \\ &\times (\{f^{(1)}(\rho)\}_i\{\hat{g}^{(1)}(\rho)\}_i^T \\ &+ \{f^{(2)}(\rho)\}_i\{\hat{g}^{(2)}(\rho)\}_i^T)\, d\rho\end{aligned} \tag{8b}$$

$$\{\hat{g}_m\}_i = \sum_{e'} \int_{e'} g_{im}(y')\{N\}_i\, dy' \tag{8c}$$

$$\{\hat{g}^{(r)}(\rho)\}_i = \sum_{e'} \int_{e'} g_i^{(r)}(\rho, y')\{N\}_i\, dy', \quad r = 0, 1, 2. \tag{8d}$$

Here δ_{i1} is the Kronecker δ, ρ is the wavenumber of the y direction in the substrate layer, and M_i is the number of guided modes in waveguide i. The components of the $\{\phi\}_i$, $\{\psi\}_i$, $\{f_m\}_i$, and $\{f^{(r)}(\rho)\}_i$ ($r = 0, 1, 2$) vectors are the values of ϕ, ψ, $f_{im}(y)$, and $f_i^{(r)}(\rho, y)$, respectively, $\{N\}_i$ is the shape function vector on Γ_i, and the superscript T denotes a transpose. A summary of the mode functions $f_{im}(y)$, $g_{im}(y)$, $f_i^{(r)}(\rho, y)$, and $g_i^{(r)}(\rho, y)$, and of the propagation constants β_{im} and $\beta_i(\rho)$ is given in the Appendix. In (8b), the integrals with respect to ρ are calculated numerically.

D. Combination of Finite and Boundary Elements

From (5), (6), and (7), we obtain the following final matrix equation:

$$\left(\begin{array}{c|c} [A'] & -[B'] \\ [H']^{(+)} & -[G']^{(+)} \\ [H']^{(-)} & -[G']^{(-)} \\ \hline [1]\,[0]\,[0]\,[0] & -[Z]_1\,[0]\,[0]\,[0] \\ [0]\,[1]\,[0]\,[0] & [0] - [Z]_2[0]\,[0] \end{array}\right) \left(\begin{array}{c} \{\phi\}_1 \\ \{\phi\}_2 \\ \{\phi\}_3^{(+)} \\ \{\phi\}_3^{(-)} \\ \hline \{\psi\}_1 \\ \{\psi\}_2 \\ \{\psi\}_3^{(+)} \\ \{\psi\}_3^{(-)} \end{array}\right) = \left(\begin{array}{c} \{0\} \\ \{0\} \\ \{0\} \\ \hline \{f\}_1 \\ \{0\} \end{array}\right) \tag{9}$$

where the components of the $\{\phi\}_3^{(\pm)}$ and $\{\psi\}_3^{(\pm)}$ vectors are the values of ϕ and ψ at the nodal points on $\Gamma_3^{(\pm)}$, respectively, [1] is a unit matrix, [0] is a null matrix, and $\{0\}$ is a null vector. The columns of $[A']$ and $[B']$ corresponding to the nodal points of Γ_F are the same as those of $[A]$ and $[B]$, respectively, and the others are zero. $[H']^{(\pm)}$ and $[G']^{(\pm)}$ are generated in the similar way from $[H]^{(\pm)}$ and $[G]^{(\pm)}$, respectively.

The solutions of (9) allow the determination of the normalized reflected power $|R_m|^2$ and the normalized transmitted power $|T_m|^2$ of the mth mode, and the normalized radiated power P_{ir} in waveguide i as follows:

$$|R_m|^2 = \frac{\beta_{1m}}{\beta_{10}} \left| \delta_{m0} + \frac{1}{-j\beta_{1m}\lambda} \{\hat{g}_m\}_1^T \{\psi\}_1 \right|^2 \tag{10a}$$

$$|T_m|^2 = \frac{\beta_{2m}}{\beta_{10}} \left| \frac{1}{-j\beta_{2m}\lambda} \{\hat{g}_m\}_2^T \{\psi\}_2 \right|^2 \tag{10b}$$

$$\begin{aligned} P_{ir} = \frac{1}{\beta_{10}\lambda} \{\psi\}_i^\dagger \Bigg(& \int_0^{k_0\sqrt{n_{i1}^2 - n_{i3}^2}} \frac{1}{\beta_i(\rho)\lambda} \{\hat{g}^{(0)}(\rho)\}_i \{\hat{g}^{(0)}(\rho)\}_i^T \, d\rho \\ & + \int_{k_0\sqrt{n_{i1}^2 - n_{i3}^2}}^{k_0 n_{i1}} \frac{1}{\beta_i(\rho)\lambda} (\{\hat{g}^{(1)}(\rho)\}_i \{\hat{g}^{(1)}(\rho)\}_i^T \\ & + \{\hat{g}^{(2)}(\rho)\}_i \{\hat{g}^{(2)}(\rho)\}_i^T) \, d\rho \Bigg) \{\psi\}_i, \qquad i = 1, 2 \end{aligned} \tag{10c}$$

where the dagger denotes Hermitian conjugate, and the integrals with respect to ρ in (10c) are calculated numerically.

IV. Computed Results

For numerical computation, introducing a parameter $D^{(+)}$, we divide the integrals with respect to y in the boundary element approach for $\Omega_B^{(+)}$ into two parts, namely,

$$\text{those in } y_3^{(+)} \le y \le D^{(+)}$$

and

$$\text{those in } D^{(+)} \le y < \infty.$$

Similarly, for $\Omega_B^{(-)}$,

$$\text{those in } -\infty < y \le -D^{(-)}$$

and

$$\text{those in } -D^{(-)} \le y \le y_3^{(-)}.$$

Also, we divide the integrals with respect to y in the analytical approach into three parts, namely,

$$\text{those in } -\infty < y \le -D^{(-)},$$

$$\text{those in } -D^{(-)} \le y \le D^{(+)},$$

and

$$\text{those in } D^{(+)} \le y < \infty.$$

Among the above integrals, the ones in $y_3^{(+)} \le y \le D^{(+)}$, $-D^{(-)} \le y \le y_3^{(-)}$, and $-D^{(-)} \le y \le D^{(+)}$ are calculated analytically, but the others are neglected by choosing the values of $D^{(+)}$ and $D^{(-)}$ adequately.

Furthermore, introducing a parameter c_i, we divide the integrals with respect to ρ in the analytical approach into three parts, namely,

$$\text{those in } 0 \le \rho \le n_{i1}k_0 \text{ (propagating part)},$$

$$\text{those in } n_{i1}k_0 \le \rho \le c_i n_{i1}k_0 \text{ (nonpropagating part)},$$

and

$$\text{those in } c_i n_{i1}k_0 \le \rho < \infty \text{ (nonpropagating part)},$$

where the first two parts are calculated numerically and the last part is neglected by choosing the value of c_i ($c_i > 1$) adequately. For simplicity, the relation $c_1 = c_2 = c$ is

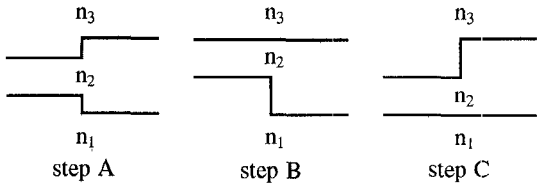

Fig. 2. Three kinds of step-discontinuities.

TABLE I
VARIATION OF SOLUTIONS WITH VALUES OF c, WHERE $D^{(+)} = 2\lambda + (d_2 - d_1)/2$ AND $D^{(-)} = 4\lambda + (d_2 + d_1)/2$

d_2/d_1	c	$\lvert R_0\rvert^2$	$\lvert T_0\rvert^2$	P_r	P_t
1.5	2	0.00003	0.93541	0.06455	0.99999
	4	0.00003	0.93540	0.06455	0.99999
2.0	2	0.00007	0.88892	0.11099	0.99998
	4	0.00007	0.88892	0.11099	0.99998

TABLE II
VARIATION OF SOLUTIONS WITH VALUES OF $D^{(+)}$, WHERE $c = 2$ AND $D^{(-)} = 4\lambda + (d_2 + d_1)/2$

d_2/d_1	$D^{(+)}$	$\lvert R_0\rvert^2$	$\lvert T_0\rvert^2$	P_r	P_t
1.5	$\lambda + 0.25\,d_1$	0.00003	0.93541	0.06454	0.99998
	$3\lambda + 0.25\,d_1$	0.00003	0.93541	0.06455	0.99999
2.0	$\lambda + 0.5\,d_1$	0.00007	0.88892	0.11098	0.99997
	$3\lambda + 0.5\,d_1$	0.00007	0.88892	0.11099	0.99998

used below. A double-exponential formula [5] is used for the numerical integration over ρ.

We consider three kinds of step-discontinuities as shown in Fig. 2, where $n_1 = 1.515$, $n_2 = 1.61$, $n_3 = 1$, $d_1 = 0.3$ μm or 0.4 μm, $\lambda = 0.6328$ μm, and the fundamental TE or TM mode incidence is assumed. Convergence of the solution should be checked on values of c, $D^{(+)}$, and $D^{(-)}$. We investigate the convergence for step A with TE mode incidence and $d_1 = 0.3$ μm.

Table I shows the variation of solutions with values of c, where P_r and P_t represent total radiated power ($P_{1r} + P_{2r}$) and total power ($|R_0|^2 + |T_0|^2 + P_r$), respectively. Since the results for $c = 2$ are almost the same as those for $c = 4$, we use $c = 2$.

Appropriate values of $D^{(+)}$ and $D^{(-)}$ are dependent on the spread of the guided mode over the y direction. Tables II and III show the variation of solutions with some values of $D^{(+)}$ and $D^{(-)}$, respectively, which are chosen in view of a field distribution of the fundamental guided mode shown in Fig. 3. From these tables, it is reasonable to decide $D^{(+)} = \lambda + (d_2 - d_1)/2$ and $D^{(-)} = 4\lambda + (d_2 + d_1)/2$.

Figs. 4 and 5 show the transmitted power and radiated power of steps A, B, and C for the TE and TM mode incidences, respectively. Our results of the radiated power of step A agree well with those of Ramaswamy and Suchoski [2]. In the case of the TE mode incidence of $d_1 = 0.4$ μm, the second-order mode ($m = 1$) exists in waveguide 2 for $d_2/d_1 \gtrsim 1.97$, and especially for step C it is strongly excited. Also, we notice that the radiated power is large in order of steps B, A, and C except for TE mode incidence of $d_1 = 0.4$ μm.

TABLE III
VARIATION OF SOLUTIONS WITH VALUES OF $D^{(-)}$, WHERE $c = 2$ AND $D^{(+)} = \lambda + (d_2 - d_1)/2$

d_2/d_1	$D^{(-)}$	$\lvert R_0\rvert^2$	$\lvert T_0\rvert^2$	P_r	P_t
1.5	$3\lambda + 1.25\,d_1$	0.00003	0.93539	0.06449	0.99991
	$5\lambda + 1.25\,d_1$	0.00003	0.93541	0.06453	0.99997
2.0	$3\lambda + 1.5\,d_1$	0.00007	0.88891	0.11094	0.99992
	$5\lambda + 1.5\,d_1$	0.00007	0.88892	0.11098	0.99997

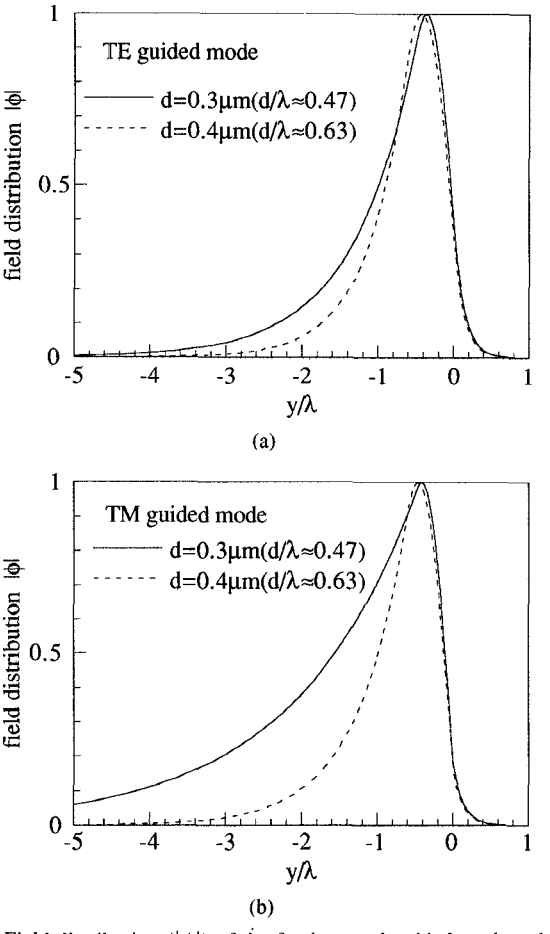

Fig. 3. Field distribution ($|\phi|$) of the fundamental guided mode, where d is waveguide thickness.

V. CONCLUSION

We have extended a combined approach of the finite-element and boundary-element methods to the analysis of discontinuities in an asymmetric slab waveguide. Here all the eigenmodes, namely guided modes, substrate radiation modes, and substrate-cover radiation modes are taken into account. Also, to show the validity and usefulness of this method, computed results have been given for three kinds of step-discontinuities with TE and TM mode in-

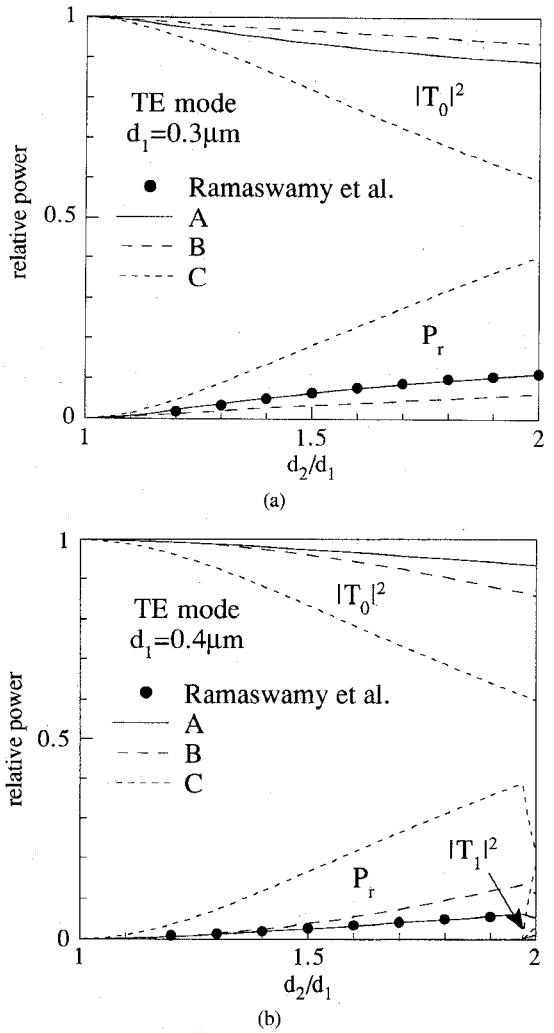

Fig. 4. Scattering characteristics of steps for TE mode incidence.

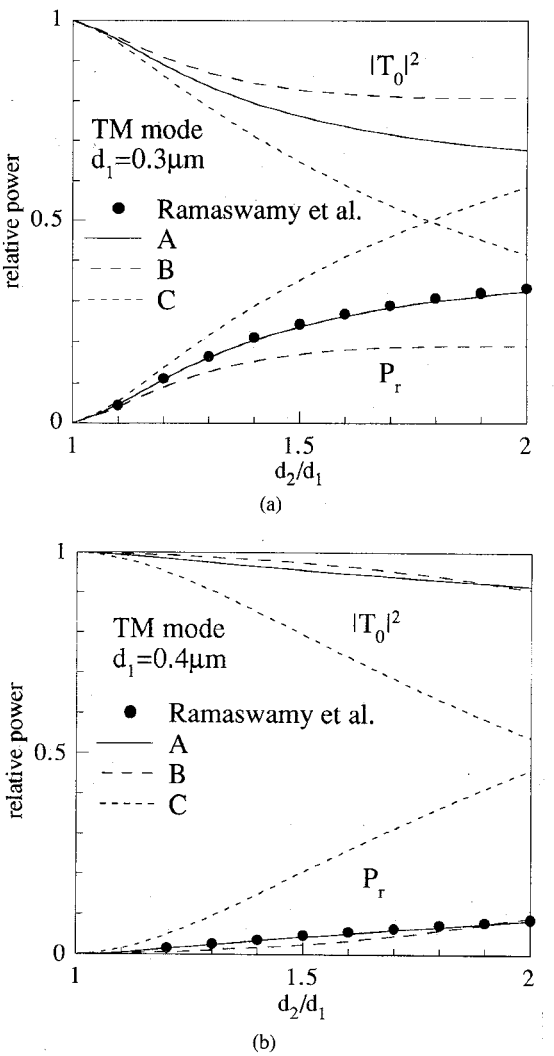

Fig. 5. Scattering characteristics of steps for TM mode incidence.

cidences. Some of the results are for the case where the second-order mode exists.

This approach can be applied to arbitrarily shaped discontinuities, and is appropriate as a solver for CAD or CAE. In the future, we intend to construct a CAE system on a workstation for the design of dielectric waveguide junctions.

Appendix

For simplicity the subscript i ($i = 1, 2$) is omitted.

A. Guided Modes

$$f_m(y) = \frac{1}{\sqrt{D_m}} h_m(y) \tag{A1}$$

$$g_m(y) = \frac{1}{\sqrt{D_m}} \frac{h_m(y)}{p(y)} \tag{A2}$$

$$D_m = \int_{-\infty}^{\infty} \frac{(h_m(y))^2}{p(y)}\, dy \tag{A3}$$

$$p(y) = \begin{cases} p_1 & (-\infty < y \le -d) \\ p_2 & (-d \le y \le 0) \\ p_3 & (0 \le y < \infty) \end{cases} \tag{A4}$$

$$h_m(y) = \begin{cases} \left(\cos \kappa_m d + \dfrac{p_2\, \delta_m}{p_3 \kappa_m} \sin \kappa_m d\right) \exp\left[\gamma_m (y + d)\right] \\ \qquad (-\infty < y \le -d) \\ \cos \kappa_m y - \dfrac{p_2\, \delta_m}{p_3 \kappa_m} \sin \kappa_m y \qquad (-d \le y \le 0) \\ \exp(-\delta_m y)\ (0 \le y < \infty) \end{cases} \tag{A5}$$

where p_j ($j = 1, 2$) is 1 for TE modes and n_j^2 for TM modes.

The dispersion relation for β_m is given as

$$\tan \kappa_m d = p_2 \kappa_m (p_2 \gamma_m + p_1\, \delta_m)/(p_1 p_3 \kappa_m^2 - p_2^2 \gamma_m\, \delta_m) \tag{A6}$$

where

$$\gamma_m = \sqrt{\beta_m^2 - n_1^2 k_0^2} \tag{A7}$$

$$\kappa_m = \sqrt{n_2^2 k_0^2 - \beta_m^2} \tag{A8}$$

$$\delta_m = \sqrt{\beta_m^2 - n_3^2 k_0^2}. \tag{A9}$$

B. Substrate Radiation Modes ($r = 0$)

$$f^{(0)}(\rho, y) = \frac{1}{\sqrt{D^{(0)}(\rho)}} h^{(0)}(\rho, y) \tag{A10}$$

$$g^{(0)}(\rho, y) = \frac{1}{\sqrt{D^{(0)}(\rho)}} \frac{h^{(0)}(\rho, y)}{p(y)} \tag{A11}$$

$$D^{(0)}(\rho)\,\delta(\rho - \rho') = \int_{-\infty}^{\infty} \frac{h^{(0)}(\rho, y) h^{(0)}(\rho', y)}{p(y)}\, dy \tag{A12}$$

$$h^{(0)}(\rho, y) = \begin{cases} \left(\cos \kappa d + \dfrac{p_2 \delta}{p_3 \kappa} \sin \kappa d\right) \cos \rho(y + d) \\ \quad + \left(\dfrac{p_1 \kappa}{p_2 \rho} \sin \kappa d - \dfrac{p_1 \delta}{p_3 \rho} \cos \kappa d\right) \\ \quad \cdot \sin \rho(y + d) \\ \qquad (-\infty < y \le -d) \\ \cos \kappa y - \dfrac{p_2 \delta}{p_3 \kappa} \sin \kappa y \qquad (-d \le y \le 0) \\ \exp(-\delta y) \quad (0 \le y < \infty) \end{cases} \tag{A13}$$

$$\beta = \sqrt{n_1^2 k_0^2 - \rho^2} \tag{A14}$$

$$\kappa = \sqrt{(n_2^2 - n_1^2) k_0^2 + \rho^2} \tag{A15}$$

$$\delta = \sqrt{(n_1^2 - n_3^2) k_0^2 - \rho^2} \tag{A16}$$

where $\delta(\rho - \rho')$ is the Dirac δ function and ρ is the wavenumber of the y direction in the substrate layer.

C. Substrate-Cover Radiation Modes ($r = 1, 2$)

Relations of $f^{(r)}$, $g^{(r)}$, and $D^{(r)}$ ($r = 1, 2$) are expressed as ones obtained by replacing the superscript 0 with r in (A10) ~ (A12).

$$h^{(r)}(\rho, y) = \begin{cases} (\cos \kappa d + C_r \sin \kappa d) \cos \rho (y + d) \\ \quad + \dfrac{p_1 \kappa}{p_2 \rho} (\sin \kappa d - C_r \cos \kappa d) \\ \quad \cdot \sin \rho(y + d) \\ \qquad (-\infty < y \le -d) \\ \cos \kappa y - C_r \sin \kappa y \qquad (-d \le y \le 0) \\ \cos \Delta y - \dfrac{p_3 \kappa}{p_2 \Delta} C_r \sin \Delta y \\ \qquad (0 \le y < \infty) \end{cases} \tag{A17}$$

$$C_1 = \sqrt{\frac{\Delta}{p_3} \cdot \frac{p_2^2 p_3 \rho^2 \cos^2 \kappa d + p_1^2 p_3 \kappa^2 \sin^2 \kappa d + p_1 p_2^2 \rho \Delta}{p_1^2 \kappa^2 \Delta \cos^2 \kappa d + p_2^2 \rho^2 \Delta \sin^2 \kappa d + p_1 p_3 \kappa^2 \rho}} \tag{A18}$$

$$C_2 = -C_1$$

$$\beta = \begin{cases} \sqrt{n_1^2 k_0^2 - \rho^2} & \text{(propagating part)} \\ -j\sqrt{\rho^2 - n_1^2 k_0^2} & \text{(nonpropagating part)} \end{cases} \tag{A19}$$

$$\kappa = \sqrt{(n_2^2 - n_1^2) k_0^2 + \rho^2} \tag{A20}$$

$$\Delta = \sqrt{\rho^2 - (n_1^2 - n_3^2) k_0^2}. \tag{A21}$$

References

[1] D. Marcuse, *Theory of Dielectric Optical Waveguides*. New York: Academic Press, 1974.

[2] V. Ramaswamy and P. G. Suchoski, Jr., "Power loss at a step discontinuity in an asymmetrical dielectric slab waveguide," *J. Opt. Soc. Am. A*, vol. 1, pp. 754–759, July 1984.

[3] K. Hirayama and M. Koshiba, "Analysis of discontinuities in an open dielectric slab waveguide by combination of finite and boundary elements," *IEEE Trans. Microwave Theory Tech.*, vol. 37, pp. 761–768, Apr. 1989.

[4] ——, "Numerical analysis of arbitrarily shaped discontinuities between planar dielectric waveguides with different thicknesses," *IEEE Trans. Microwave Theory Tech.*, vol. 38, pp. 260–264, Mar. 1990.

[5] H. Takahasi and M. Mori, "Double exponential formulas for numerical integration," *Publications of the Research Institute for Mathematical Science*, Kyoto University, vol. 9, pp. 721–741, 1974.

Koichi Hirayama (M'89) was born in Shiranuka, Hokkaido, Japan, on September 8, 1961. He received the B.S., M.S., and Ph.D. degrees in electronic engineering from Hokkaido University, Sapporo, Japan, in 1984, 1986, and 1989, respectively.

In 1989, he joined the Department of Electronic Engineering, Kushiro National College of Technology, Kushiro, Japan, where he became an Associate Professor in 1991. His research interests include the analysis of discontinuities problems in an open dielectric waveguide.

Dr. Hirayama is a member of the Institute of Electronics, Information and Communication Engineers (IEICE).

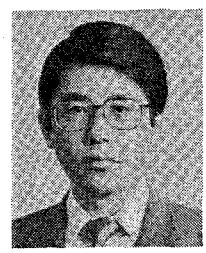

Masanori Koshiba (SM'84) was born in Sapporo, Japan, on November 23, 1948. He received the B.S., M.S., and Ph.D. degrees in electronic engineering from Hokkaido University, Sapporo, Japan, in 1971, 1973, and 1976, respectively.

In 1976, he joined the Department of Electronic Engineering, Kitami Institute of Technology, Kitami, Japan. From 1979 to 1987, he was an Associate Professor of Electronic Engineering at Hokkaido University, where he became a Professor in 1987. He has been engaged in research on lightwave technology, surface acoustic waves, magnetostatic waves, microwave field theory, and applications of finite-element and boundary-element methods to field problems.

Dr. Koshiba is a member of the Institute of Electronics, Information and Communication Engineers (IEICE), the Institute of Television Engineers of Japan, the Institute of Electrical Engineers of Japan, the Japan Society for Simulation Technology, and the Japan Society for Computational Methods in Engineering. In 1987, he was awarded the 1986 Paper Award by the IEICE.